Excited State Dynamics of 1,4-diphenyl-1,3-butadiene and
1,1,4,4-tetraphenyl-1,3-butadiene Probed by Time-Resolved Electronic Spectroscopy

A Senior Honors Thesis

Presented in Partial Fulfillment of the Requirements for graduation *with research distinction* in
Chemistry in the undergraduate colleges of The Ohio State University

by

Jessica Erin Donehue

The Ohio State University
June 2009

Project Advisor: Terry L. Gustafson

ABSTRACT

The visual pigment 11-*cis*-retinal is covalently bonded to Lys-296 of the heptahelical membrane protein rhodopsin through a protonated Schiff base linkage. Photoisomerization of this chromophore induces a structural change in the protein that initiates the vision process. Studies have found this isomerization process occurs inside the protein in about 200 femtoseconds. Considering the relative size of the chromophore, its constrained environment, and the way in which a molecule is traditionally considered to rotate during the isomerization process, this time constant is surprisingly fast. Even more intriguing is that in solution, where the chromophore is free from the constraints of the protein, the time constant for the rate of isomerization increases dramatically to 3 picoseconds. Though it is generally accepted the surrounding protein catalyzes the rapid rate of isomerization, the mechanism by which this occurs is not well understood. Volume-conserving mechanisms of photoisomerization, such as the bicycle pedal (BP) and the Hula-twist (HT) have been proposed to explain this enhanced rate. However, little experimental data is available to support this claim. This project proposes to unveil the mechanisms of isomerization in constrained environments. A sterically hindered derivative of 1,4-diphenyl-1,3-butadiene (DPB), 1,1,4,4-tetraphenyl-1,3-butadiene (TPB) will be employed to understand the mechanism of photoisomerization in constrained environments. Through the use of femtosecond transient absorption spectroscopy and picosecond spectroscopy, we will investigate the excited state dynamics of TPB and compare the results to previously studied DPB. From this, we hope to gain new information about the influence of structural details and solvent environment on the isomerization process.

AKNOWLEDGEMENTS

Many thanks go to my advisor, Terry L. Gustafson, for his encouragement, reassurance, and great scientific insight. Without him, I would have never realized my great love of laser spectroscopy.

I would also like to thank the Kohler group members, especially, Joe Henrich, Kimm de la Harpe, and Charlene Su. Though I was not your undergrad, you offered your wisdom and your time to help me whenever I needed experimental guidance or understanding of the vast world of physical chemistry.

Finally, more thanks than I could ever put into words go to Nicole Dickson. I truly am a better scientist today for having the chance to work with you on this project. Your devotion to research and your investment in teaching those who work alongside you make you a rare gem in the scientific world. I am honored to have worked with you for the last two years, and one day the world will know just how awesome the two of us are.

TABLE OF CONTENTS

Chapter 1

INTRODUCTION

1.1 Photoisomerization in Retinal

At the back of the mammalian eye lies the retina. This light-sensing tissue consists of a thin layer of cells and is approximately 0.25 mm thick. Inside these cells resides the protein rhodopsin, which surrounds the chromophore 11-*cis*-retinal. This chromophore is covalently bonded to Lys-296 of the heptahelical membrane protein rhodopsin through a protonated Schiff base linkage. Upon absorption of a photon, the 11-*cis*-retinal molecule undergoes photoisomerization to 11-*trans*-retinal, which induces a structural change in the chromophore. This structural change is the first step in a cascade of events that initiate the vision process[1]. Studies on the excited state photophysics of retinal have found this isomerization process to occur on a time scale of approximately 200 femtoseconds (fs)[2,3]. Considering the relative size of the chromophore, its constrained environment, and the way in which a molecule is conventionally considered to rotate during the isomerization process, this time constant is surprisingly fast. Even more intriguing is that when the chromophore is removed from the constraining protein environment and placed in free solution, the time constant for the rate of isomerization increases dramatically to 3 picoseconds (ps)[4].
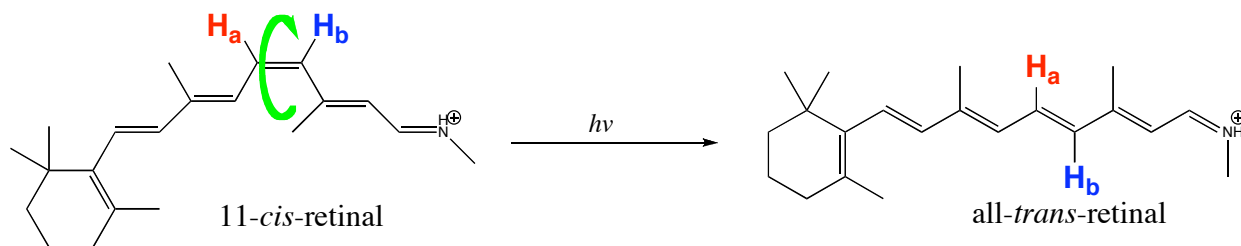

Figure 1.1. *cis-trans* isomerization of retinal upon absorption of a photon.

Though it is generally accepted that the surrounding protein catalyzes the rapid rate of isomerization, the mechanism by which this occurs is not well understood. The one-bond-flip is the most accepted mechanism of isomerization and involves a torsional motion around a double bond. This movement, however, is very large in amplitude and very volume demanding, resulting in a long lifetime. Volume-conserving mechanisms of photoisomerization such as the bicycle pedal (BP)[5] and the Hula-twist (HT)[6] have been proposed to explain this enhanced rate of isomerization. These mechanisms are expected to reduce the volume requirements associated with isomerization of the molecule. This occurs through confining most of the motion to the isomerizing bonds, while the motion of bulky substituents is minimized.

1.2 Volume-Conserving Isomerization Mechanisms

In the BP mechanism, a molecule undergoes bond inversion in the excited state. After this inversion, rotation takes place simultaneously about the two bonds that were previously double bonds in S_0. Warshel first proposed this mechanism after a series of molecular dynamics simulations of retinal during its photoisomerization inside the protein cavity and monitoring the conformational changes of the chromophore as a function of time. This model was one of the first to reproduce the main experimental observations of the photoisomerization process.

Warshel's model used a method for evaluation of the vibronic transition intensities that accurately calculated the resonance Raman (RR) spectrum inside the protein cavity. The main features of the RR spectra of Schiff bases of retinal in solution were also accurately reproduced using the model. Experimentally observed red-shifts in the absorption spectra during the *cis-trans* isomerization process were also accurately predicted using the Warshel model [5].

More recently, Saltiel and co-workers have proposed that the photoisomerization of solid-state *cis,cis*-1,4-diphenyl-1,3-butadiene (DPB) to *trans,trans*-DPB proceeds via the BP mechanism. The *trans,trans* isomer was the sole product observed in the solid-state reaction and the two-bond photoisomerization was explained by Warshel's BP mechanism. This sole product was the result of the edge to face phenyl-phenyl interactions that occur in the solid-state. These interactions anchor the phenyl rings, therefore increasing the probability of a volume-conserving mechanism to take place. This study proposed the reaction proceeds in stages that are possibly due to the difference in reactivity of the two conformers and could be further influenced by changes in the crystal environment[7].

The HT mechanism involves an out-of-plane 180º rotation of a single CH unit, while the remaining portions of the molecule slide along in the direction of the plane of the molecule. Liu and Hammond first proposed this model in 1985 as a photoisomerization pathway for polyene chromophores imbedded in a protein binding cavity, such as retinal, or other rigid medium[8]. Their work, however, does suggest the dominant pathway in fluid medium is the commonly accepted one-bond-flip mechanism. Liu and Hammond propose the HT mechanism for retinal based on the distribution of products from the photoisomerization of retinal in the protein cavity. Because the 13-*cis* isomer is not observed as a photoproduct from rhodopsin, they believe the binding site in the protein is highly restrictive near the Schiff-base linkage of retinal. The 7-*cis* isomer is also not observed as a photoproduct suggesting the ring terminus of the chromophore is also restricted inside the cavity. This leaves a loose pocket of the binding site that is specifically localized in the region surrounding the C-10 and C-11 bonds of the chromophore. With this picture of the local molecular environment of the chromophore within the protein, Liu and Hammond propose the HT is responsible for the rapid rate of isomerization[6].

Experimentally, Liu and Hammond propose the HT as the process responsible for the *trans* to *cis* isomerization of the recently discovered photosensitive pigment photoactive yellow protein (PYP). This process has demonstrated a preference for isomerization at the smaller thioester end of the double bond, as opposed to the larger phenoxide ring. Liu and Hammond suggest that because the protein is confined within a rigid matrix the HT is the process responsible for this product preference[9].
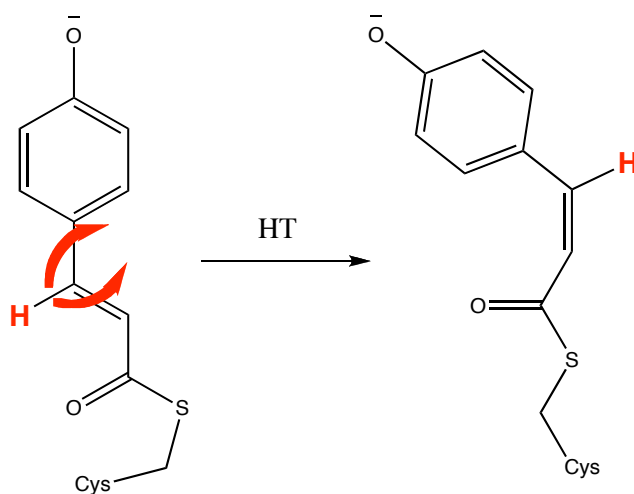

Figure 1.2. *trans-cis* isomerization of PYP via HT mechanism, adapted from Lui and Hammond's work.
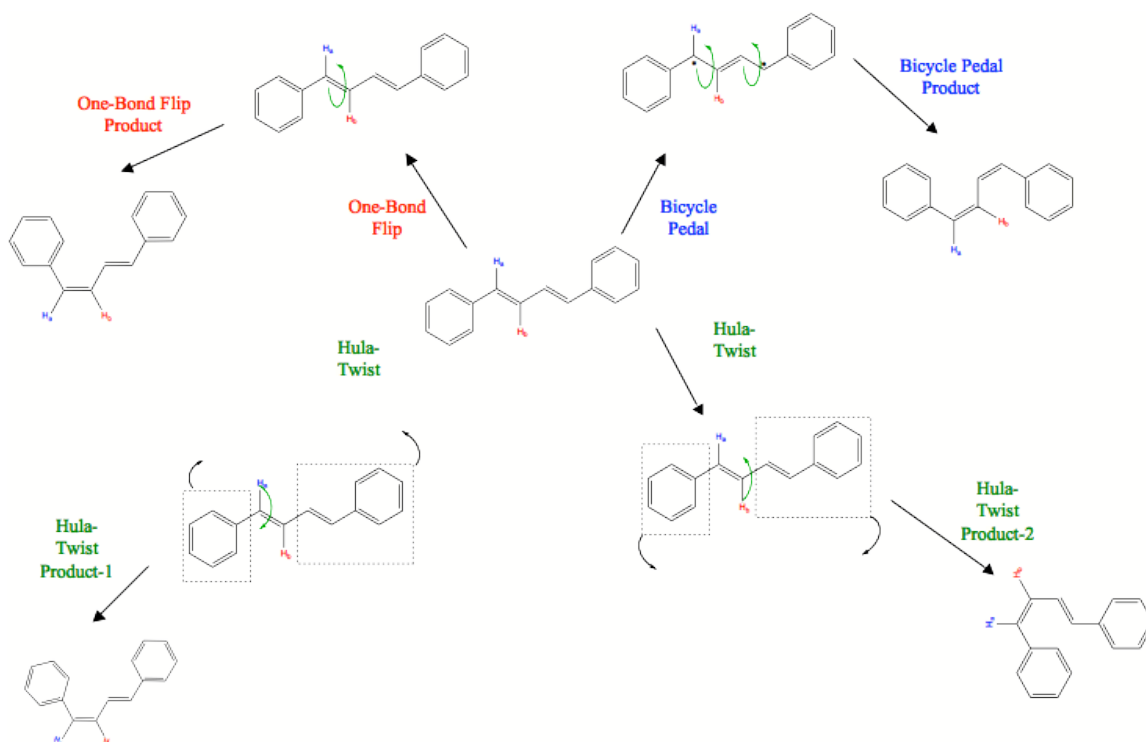
Figure 1.3. Three possible mechanisms for photoisomerization shown using 1,4-diphenyl-1,3-butadiene as an example molecule. One product results from either the one-bond flip or the bicycle pedal process; however, the Hula-twist can yield two different products, depending on which CH unit rotates 180° out-of-plane.

1.3 Model Systems for Biological Molecules

In order to study the molecular processes of large biological molecules, like the enhanced photoisomerization of retinal, smaller model systems are often used. α,ω-diphenylpolyenes with the general formula Ph-(HC=CH)$_n$-Ph, such as 1,4-diphenyl-1,3-butadiene (n=2) have been extensively studied as model compounds for larger biological polyene molecules due to their similar structure, excited state symmetries and known photoisomerization pathways.
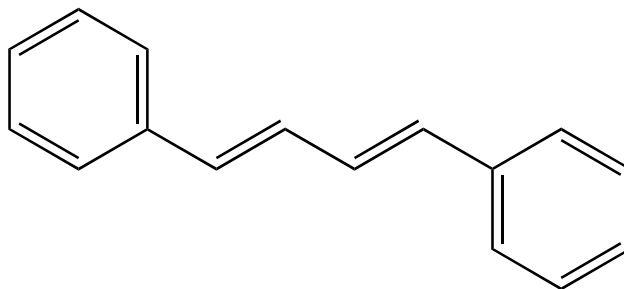
Figure 1.4. Structure of the model molecule, 1,4-diphenyle-1,3-butadiene

The ground state symmetry of these molecules is of 1Ag symmetry, while the first and second excited states are of 1^1B_u and 2^1A_g symmetry. The first two excited states of 1,4-diphenyl-1,3-butadiene (DPB) are very close in energy and nearly degenerate. Their order, as well as the energy gap between them, has been shown to be dependent on solvent environment.

Previously, Shepanski *et al.* have used one and two-photon spectroscopy to study the excited state ordering of DPB. Results from these studies suggest the lowest excited-state is of ^1A_g symmetry[10]. However, fluorescence studies done by Velsko *et al.* have shown the emitting state and the absorbing state are not of different character, suggesting the lowest excited state is of ^1B_u symmetry[11]. Also, Raman spectra collected by Morris *et al.* suggest the lowest excited state contains both ^1A_g and ^1B_u character[12,13].

It is well accepted that upon absorption of a photon, DPB is excited to the ^1B_u state, where the molecule undergoes bond order inversion[14]. From this excited state, the molecule is able to relax through nonradiative photoisomerization. For this reason, DPB is an ideal model for studying the dependence of the rate of photoisomerization on solvent environment.

Once the state in which photoisomerization takes place is identified, time-resolved techniques can be used to assign time constants to the process. With this assignment, the rate of photoisomerization in DPB, which is described in many studies[15], can be used to understand the

excited state processes of less studied molecules, like the sterically-hindered DPB derivative 1,1,4,4-tetraphenyl-1,3-butadiene (TPB).
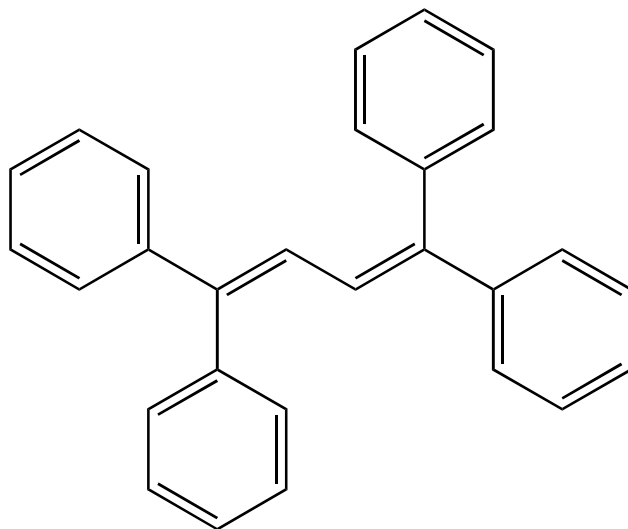

Figure 1.5. Structure of the model molecule, 1,1,4,4-tetraphenyle-1,3-butadiene

Few studies have been done on TPB and very limited information about its excited state dynamics is available. Little is known about the order of the excited states of TPB, but due to its extended effective conjugation, these states are likely to lie further apart than those of DPB. El-Bayoumi *et al*. reported the absorption and emission spectra of TPB in various hydrocarbon solvents at room temperature and in a rigid glass at 77 K. This study found the equilibrium geometry of the excited state to be different from that of the ground state and suggested intramolecular twisting as the main decay pathway[16]. Rucker *et al.* preformed picosecond (ps) transient absorption experiments and found TPB demonstrated a viscosity-independent lifetime of approximately 1.7 ps[17].

Though these previously reported results might seem to suggest TPB is a simple molecule with limited value, it provides a wonderful model system for investigating the effect of steric hindrance on excited state dynamics, specifically photoisomerization. By comparing its

dynamics to those of DPB, the role of the extra phenyl rings in the excited state can be understood.

In this thesis, we propose to use picosecond time-resolved and femtosecond time-resolved spectroscopies to study the decay pathways of the sterically hindered TPB. We believe the hindered nature of TPB will model the constrained environment of retinal inside the protein cavity. With this model, we hope to induce a volume-conserving isomerization mechanism and study its validity as a mechanism in constrained environments. We will also use two homologous solvent series to further constrain the probe molecule at increasing degrees of viscosity. Our study will provide new information on how specific structural details and solvent environment influence the isomerization process. We expect to observe pathway dependent time constants indicative of the isomerization mechanism.

Chapter 2

EXPERIMENTAL METHODS

2.1 Sample Preparation

The 1,4-diphenyl-butadiene (DPB) (Kodak, scintillation grade) and 1,1,4,4-tetraphenyl-1,3-butadiene were used without further purification The solvents used were ethanol, decanol, hexanol, methanol, decane, heptane, hexane, and octane. All solvents were used as received. Sample concentrations were 10^{-5}-10^{-6} M.

2.2 Steady-State Spectroscopy

All steady-state experiments were done at room temperature in a 1 mm quartz cuvette. Absorption spectra were collected on a UV/Vis spectrometer (Perkins-Elmer Lamda 20) in each solvent before and after each broadband and kinetic experiment to ensure no formation of photoproducts and no sample degradation. Samples were scanned from 200 nm to 500 nm. Fluorescence spectra were collected on a fluorimeter (Jobin Yvon Fluorolog 2) in each solvent. Samples were excited at 310 nm and scanned from 350 nm to 550 nm. The zero-zero transition was determined by the point at which the absorption and fluorescence spectra crossed.

2.3 Femtosecond Laser System

Transient absorption lifetime decays and broadband spectra were collected using an ultra-fast femtosecond (fs) laser system. Briefly, a Ti:Sapphire oscillator and regenerative amplifier generate ~50 fs pulses, which are centered at 800 nm. The light exiting the regenerative amplifier is split, sending more than half to two optical parametric amplifiers, a UV-Vis and an SFG model, and the rest bypasses the OPA to be used as the probe beam.

The light exiting the OPA is sent through a CaF_2 half waveplate and then a polarizer, which is set at magic angle (54.7°). From the polarizer, the pump beam is "chopped," blocking two of each set of three pulses that pass through. This optical chopper acts as a trigger source for the lock-in amplifier. Signal is obtained when both the pump and probe are present at the sample. When the pump is blocked, and only the probe is present, the lock-in reads this as the reference. The lock-in also eliminates much of the noise present from the electrical systems and vibrations, which could interfere with measurements.

The light by-passing the OPA is sent through an optical delay that is controlled on a translational stage. After the optical delay, the light is sent through a water cell (kinetics detection) or a CaF_2 cell (broadband detection) to generate white light continuum. This stage is nonlinearly scanned in time several times per sample until good signal-to-noise is achieved. This white light is used as the probe.

In broadband experiments, a filter is used after the sample to block some of the pump beam, so that the CCD detector is not saturated. In kinetic detection experiments, band pass filters are used to select the "single" wavelength of the probe beam that the detector (a joule meter) monitors.

2.4 Femtosecond Time-Resolved Spectroscopy

Transient absorption experiments are used to probe the excited states of molecules. Unlike fluorescence experiments, transient absorption experiments are not limited to observing only fluorescing states. This technique allows for the observation of so-called "dark states" and, therefore, offers a more thorough view of the excited state dynamics in a particular system. In broadband transient absorption experiments, a full spectrum of the various excited states of a

14

molecule is collected. In kinetic detection experiments, a filter is used in order to monitor a "single" wavelength (though the bandpass filters are approximately ten nm wide). In both types of experiments, pump-probe techniques were utilized in collecting the excited state spectra. This technique consists of a pump pulse that initially excites the molecule of interest to the excited state. A second probe pulse is then used to excite the molecule from the excited state to a higher-energy S_n state after a carefully defined delay through use of a computer-controlled delay stage. Data collected in these experiments is analyzed from a plot of intensity versus time.

Broadband transient absorption measurements of DPB were collected at a pump wavelength of 350 nm. The solvents used for this molecule were acetonitrile, ethanol, decane, hexane, hexanol, methanol, and octane. Broadband spectra of TPB were collected using a pump wavelength of 310 nm. The solvents used for this molecule were decanol, ethanol, and hexane. The detection system consisted of a CCD camera, which was calibrated such that data was collected between roughly 370 nm and 710 nm. A flowing sample cell was used to prevent re-excitation of the sample population, which could lead to photoproduct formation. In the kinetic detection experiments, a low-volume sample cell was spun at several rpm for the same reason.

Kinetic detection experiments were collected using the solvents mentioned previously. For experiments done with DPB, 310 nm and 350 nm were used as pump wavelengths. Probe wavelengths of 570 nm, 630 nm, and 700 nm were used. For experiments done with TPB, 295 nm and 385 nm were used as pump wavelengths, while a probe wavelength of 650 nm was used.

2.5 Time-Correlated Single Photon Counting

Time-correlated single-photon counting (TCSPC) is an effective method of measuring accurate fluorescence lifetimes and was used in this thesis to conduct time-resolved

fluorescence experiments on DPB and TPB. Generically, a TCSPC measurement is obtained through excitation of a sample, collecting a photon emitted by the sample, and then measuring the period of time between these two events. More specifically, experiments for this thesis were done on a laser system that consists of a Nd:YLF laser, which is used to pump a cavity dumped rhodamine 6G dye laser to generate 580 nm pulses. This pulse train is frequency doubled to 290 nm, and a UV polarizer is used to polarize the UV light, before the beam is focused near the front of the quartz sample cell. The fluorescence emission is collected 90° to the excitation beam, where it goes through a second polarizer set at either parallel, perpendicular, or magic angle (54.7°) to the excitation light. The fluorescence is then sent through a polarization scrambler to remove any effects of polarizing the emission and focused on a subtractive-dispersive double monochromator and detected by a multichannel plate photomultiplier tube. The experiments done in this thesis were collected in "reverse mode," meaning the emission from the sample provided the "start" pulse to the time-to-amplitude converter (TAC). The 580 nm light generated by the dye laser is sent to a photodiode and acts as a stop pulse for the TAC. The TAC capacitance is sent to a multichannel analyzer, where the data is binned and displayed as a histogram, which represents the fluorescence decay. Experiments were done in reverse mode to prevent "pulse pileup". This occurs because the first photons to arrive at the TAC stop the measurement, causing the fluorescence measurement to appear shorter than it actually is.
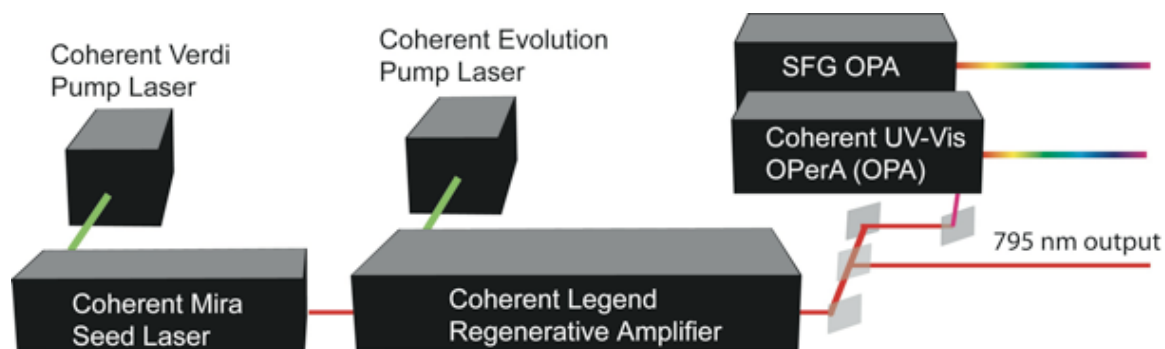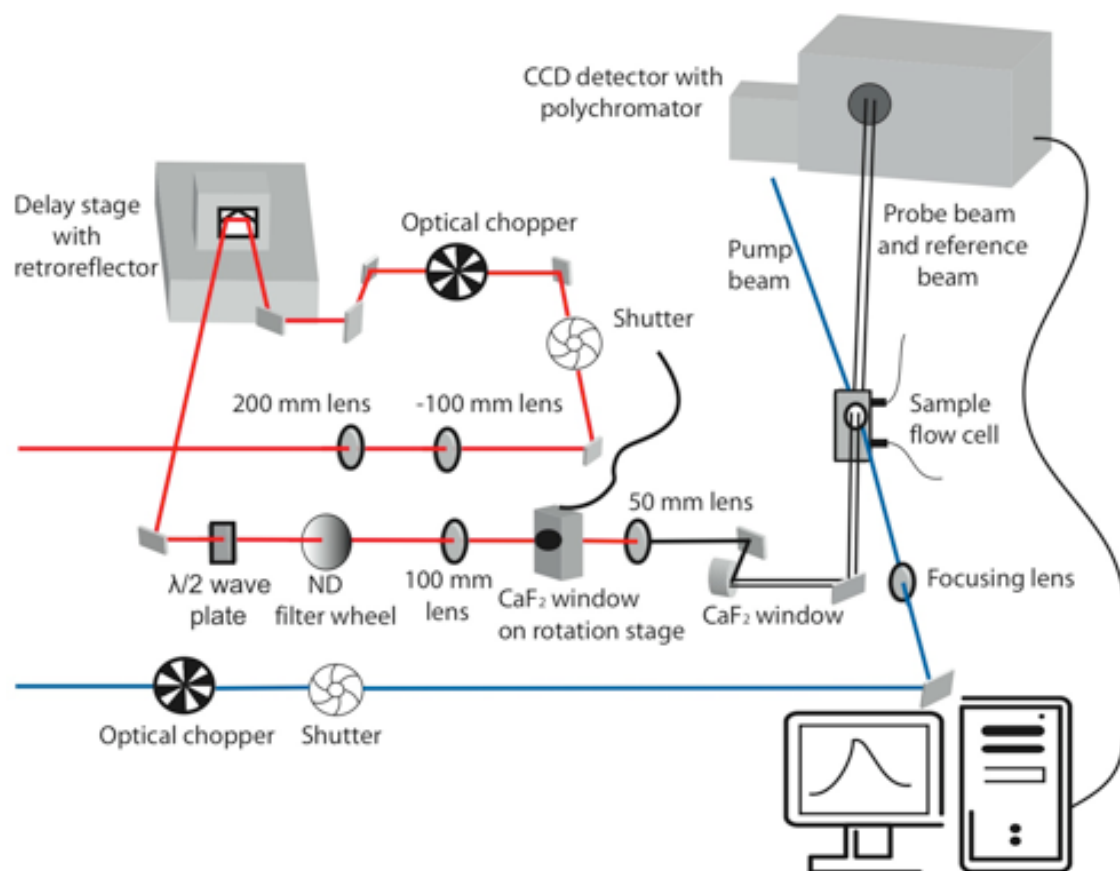
Figure 2.1. Set-up for femtosecond laser system.

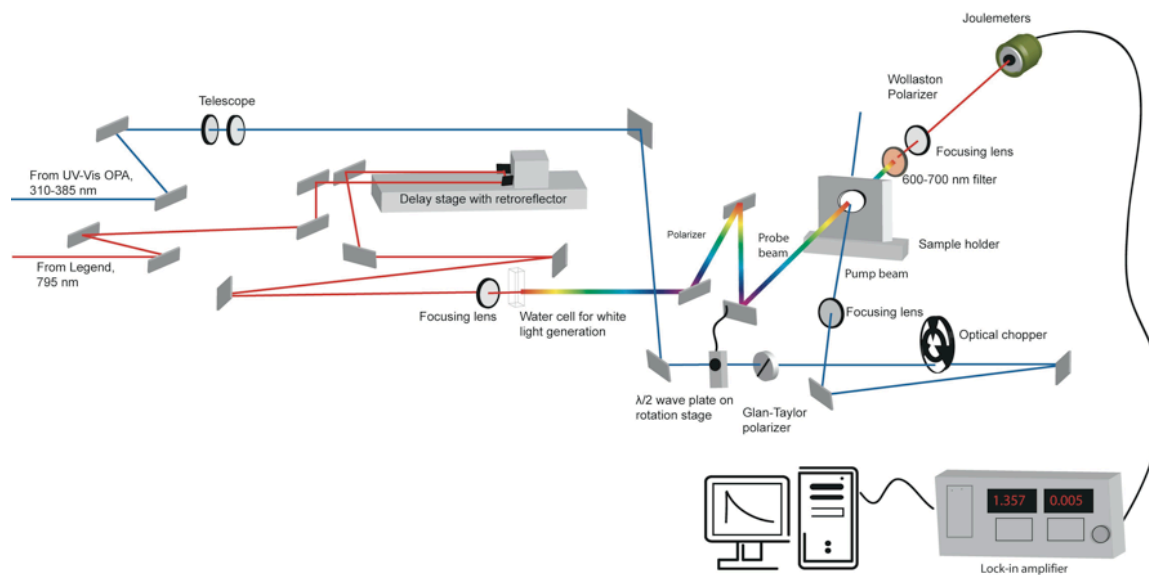**Figure 2.2.** Set-up for transient absorption broadband experiments.

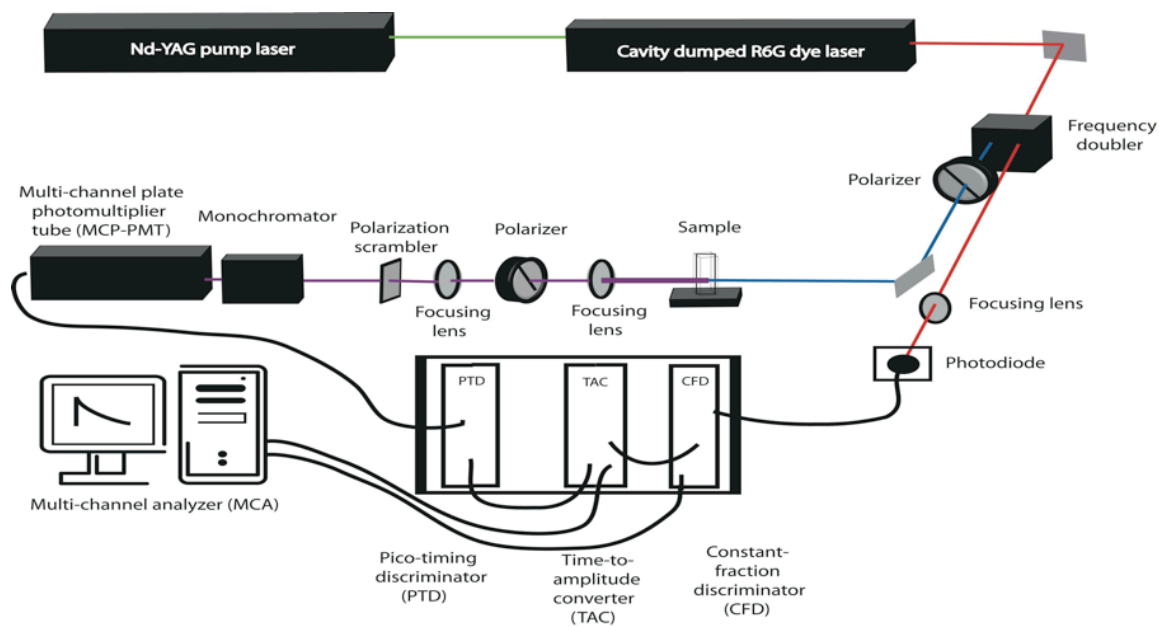**Figure 2.3.** Set-up for transient absorption single-wavelength kinetics experiments.

Figure 2.4. Set-up for time-correlated single-photon counting experiments.

Chapter 3

RESULTS

3.1 Steady-State Spectroscopy

Absorption, emission, and transient absorption spectra of DPB and TPB in ethanol were collected and are compared in Figure 3.1. The figure shows that the spectra of TPB are red-shifted in comparison to the spectra of DPB.
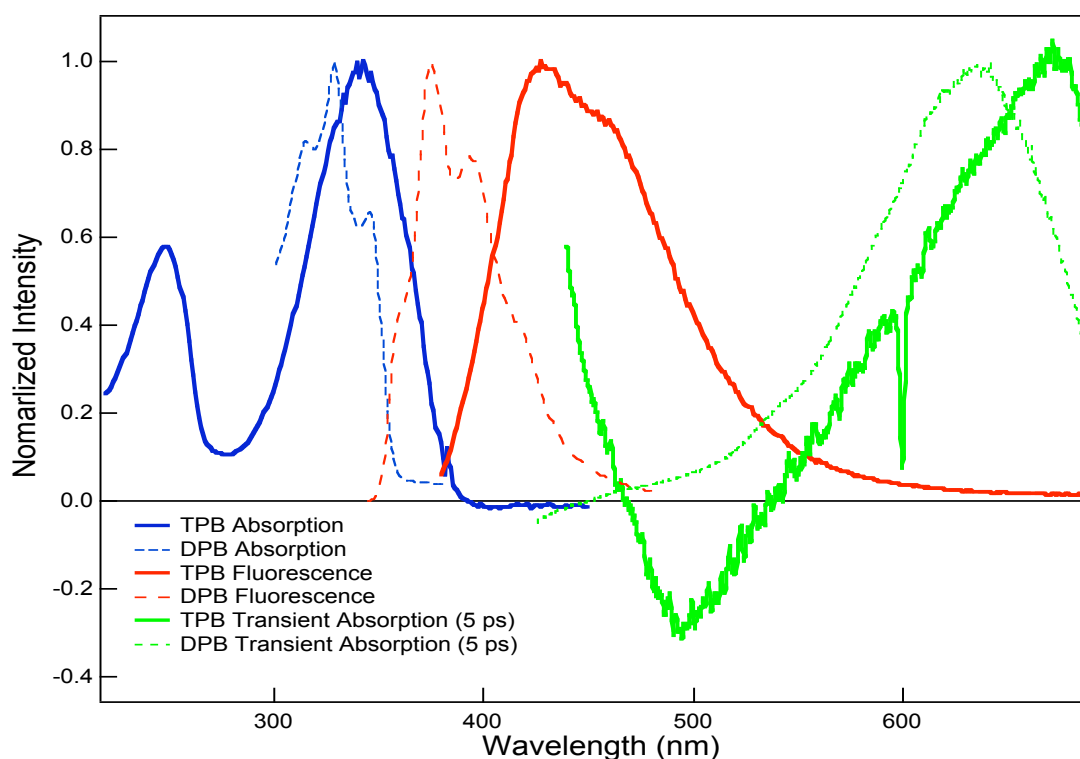

Figure 3.1. Absorption, emission, and transient absorption of DPB (broken lines) and TPB (solid lines).

3.2 Femtosecond Time-Resolved Spectroscopy

The transient absorption lifetimes for DPB in acetonitrile, ethanol, decane, decanol, hexane, hexanol, methanol, and octane were obtained with a pump wavelength of 350 nm and

were probed at 630 nm, which is approximately the maximum of the transient absorption. Figure 3.2 shows the transient absorption lifetime decays of DPB in methanol, acetonitrile, hexane, and hexanol. Each of these lifetimes was fit to a double-exponential decay. The decays show an increase in lifetime across a homologous solvent series with increasing viscosity. The decay kinetics were also observed with a pump wavelength of 310 nm and a probe wavelength of 630 nm. Within experimental error, no change was observed in the decay kinetics at higher pump energy.

The transient absorption lifetimes for TPB in methanol, ethanol, hexanol, decanol, hexane, heptane, octane, and decane were obtained with pump wavelengths of 385 nm and 295 nm, with a probe wavelength of 650 nm (approximately maximum of transient absorption) for each pump wavelength. Figures 3.3 and 3.4 show the transient absorption lifetime decays for TPB in a homologous alcohol and homologous alkane solvent series, respectively, at a pump wavelength of 295 nm. Figures 3.5 and 3.6 show similar transient absorption lifetime decays for TPB at a pump wavelength of 385 nm. The decays in the alcohol series at each pump wavelength were fit to triple-exponential decays, while the decays in the alkane series were fit to double-exponential decays. At both pump wavelengths, the decays show an increase in lifetime across a homologous solvent series with increasing viscosity.

Figures 3.7 and 3.8 show a comparison between the transient absorption decays of DPB and TPB in ethanol and hexane, respectively. Tables 1.1 and 1.2 also show a comparison of the two molecules across the solvent series, as well as the two pump wavelengths. As seen in the figures, the TPB decay in ethanol exhibits a femtosecond component not seen in that of DPB. The tables show the τ_2 component in TPB is shorter than that of DPB. The τ_3 component, however, is comparable between the two molecules and is similar in magnitude.
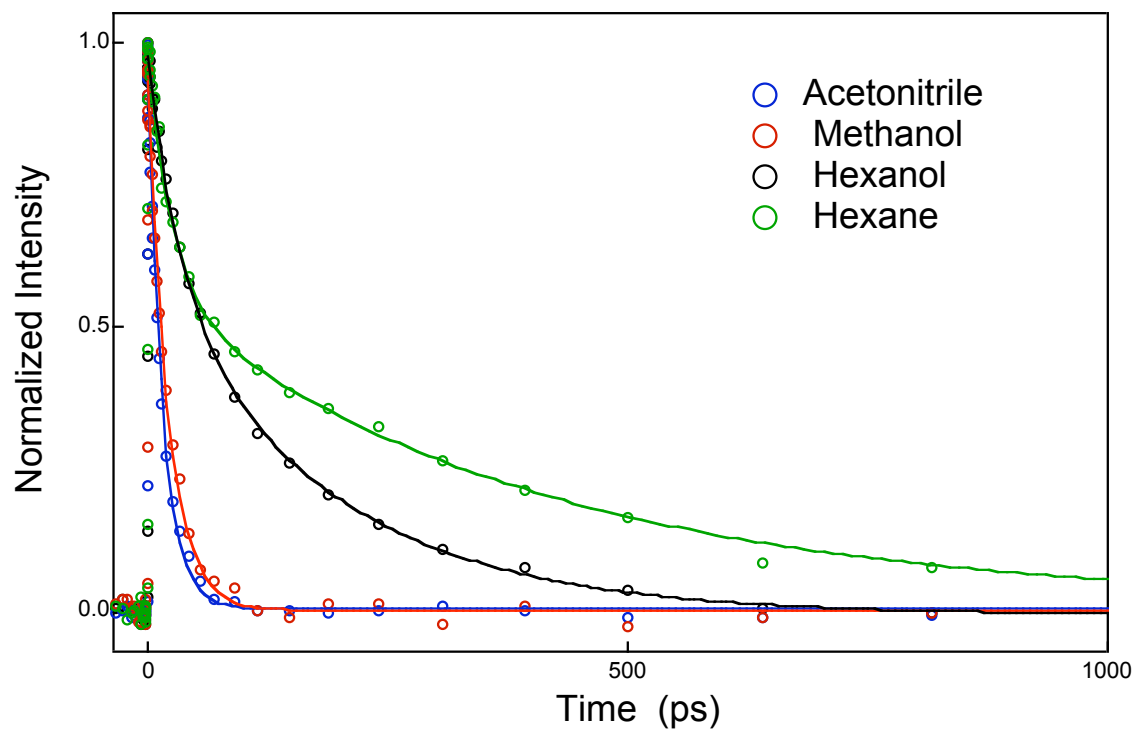
Figure 3.2. Transient absorption lifetime decays of DPB in acetonitrile, methanol, hexanol, and hexane. The pump wavelength used was 350 nm and the probe wavelength was 630 nm. The solid lines are the best fit lines to the decays. Hexane and hexanol have been fit to double-exponential decays, while acetonitrile and methanol have been fit to single-exponential decays.

Figure 3.3. Transient absorption lifetime decays of TPB in methanol, ethanol, hexanol, and decanol. The pump wavelength used was 295 nm and the probe wavelength was 650 nm. The solid lines are the best fit lines to the decays. All four solvents have been fitted to triple-exponential decays. Inset shows close-up of the first 20 ps of the decay.

Figure 3.4. Transient absorption lifetime decays of TPB in hexane, heptane, and decane. The pump wavelength used was 295 nm and the probe wavelength was 650 nm. The solid lines are the best fit lines to the decays. All three solvents have been fitted to double-exponential decays. Inset shows close-up of the first 20 ps of the decay.
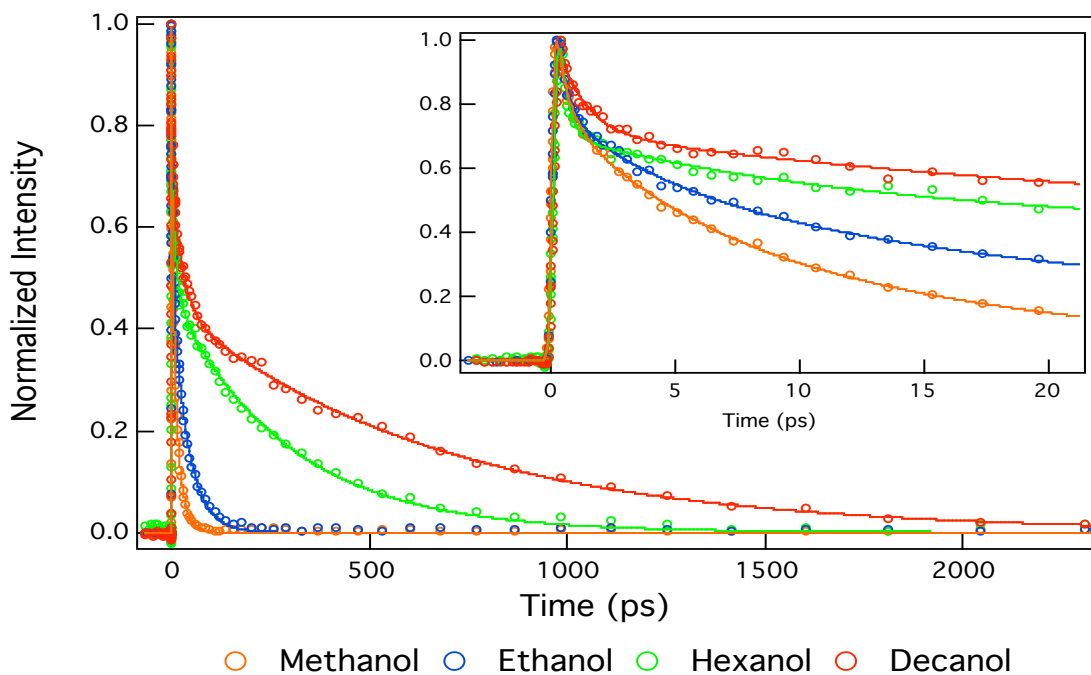
Figure 3.5. Transient absorption lifetime decays of TPB in methanol, ethanol, hexanol, and decanol. The pump wavelength used was 385 nm and the probe wavelength was 650 nm. The solid lines are the best fit lines to the decays. All four solvents have been fitted to triple-exponential decays. Inset shows close-up of the first 20 ps of the decay.
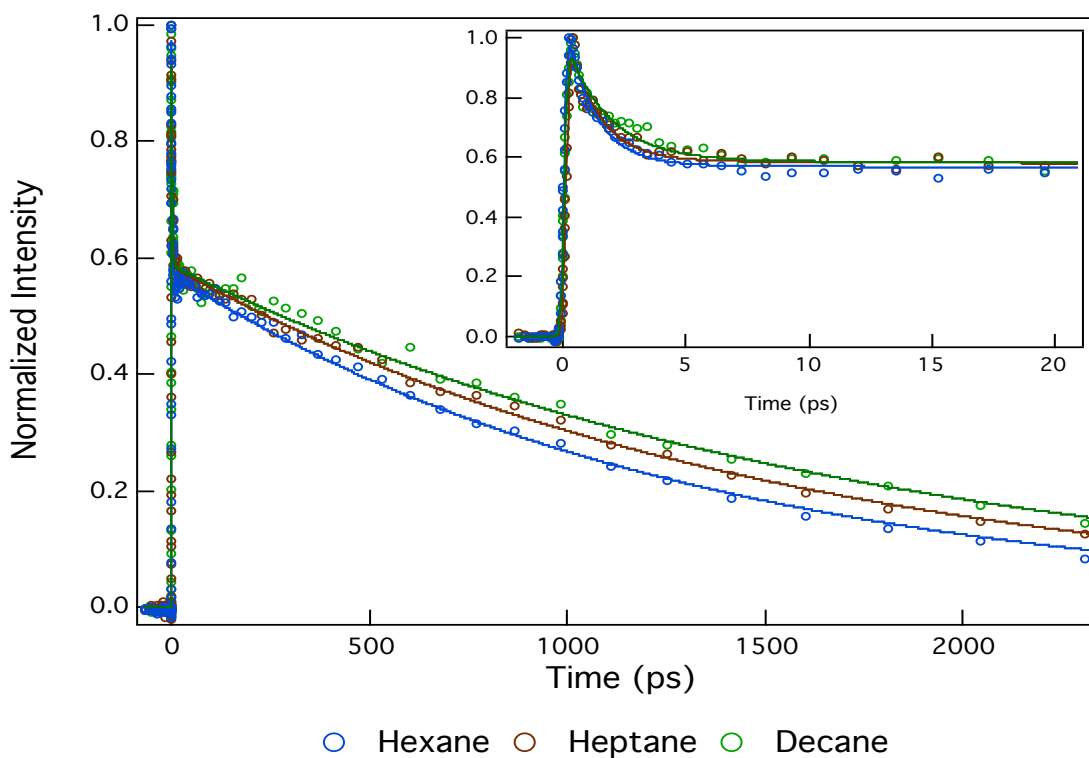
'
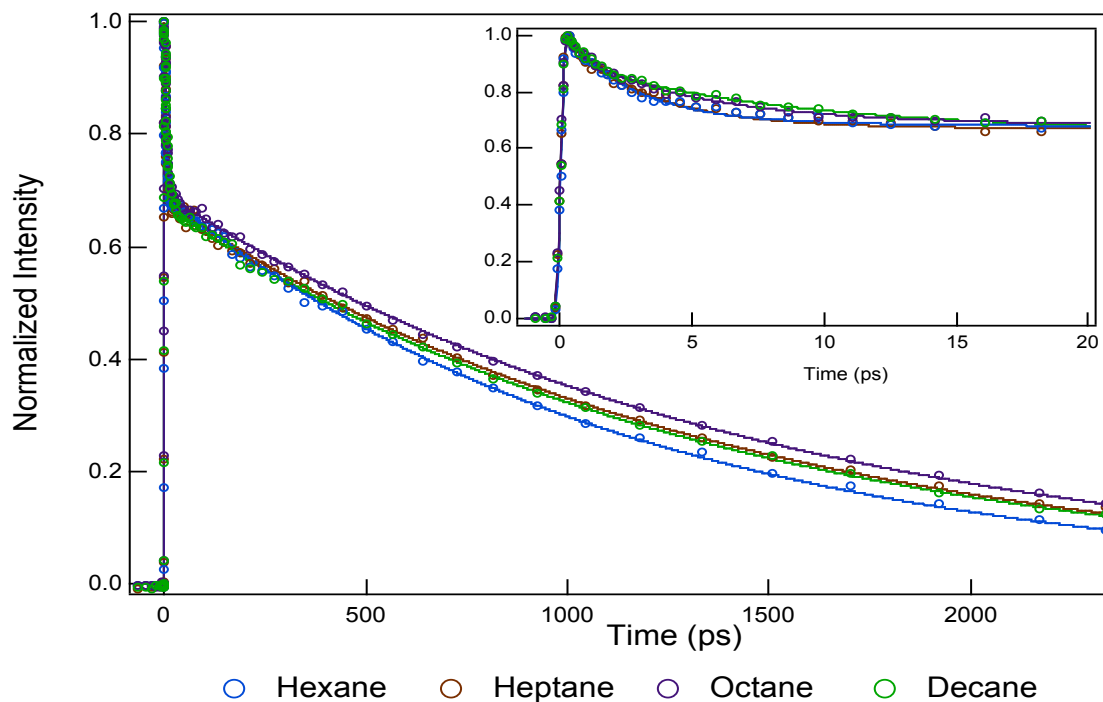
Figure 3.6. Transient absorption lifetime decays of TPB in hexane, heptane, octane, and decane. The pump wavelength used was 385 nm and the probe wavelength was 650 nm. The solid lines are the best fit lines to the decays. All four solvents have been fitted to double-exponential decays. Inset shows close-up of the first 20 ps of the decay.
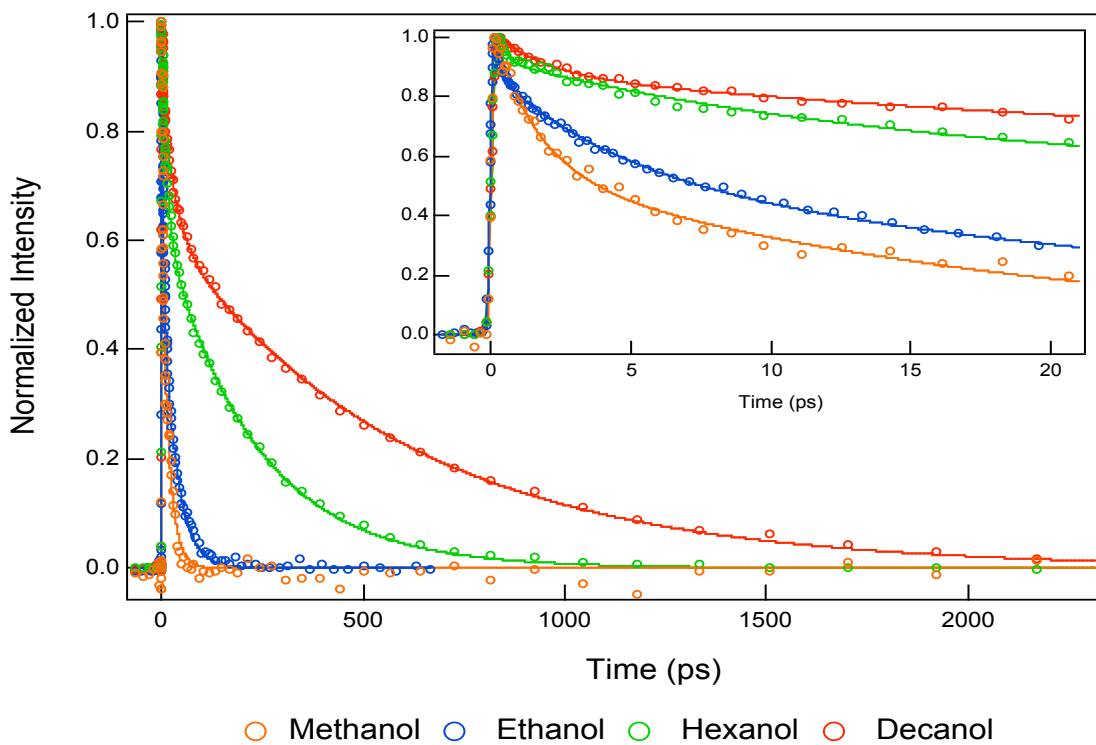
Figure 3.7. Transient absorption lifetime decays of TPB and DPB in ethanol. The pump wavelengths used were 385 nm and 350 nm, respectively, with probe wavelengths of 650 nm and 630 nm, respectively. The solid lines are the best fit lines to the decays. The decay of TPB was fit to a triple-exponential, while that of DPB was fit to a double exponential.
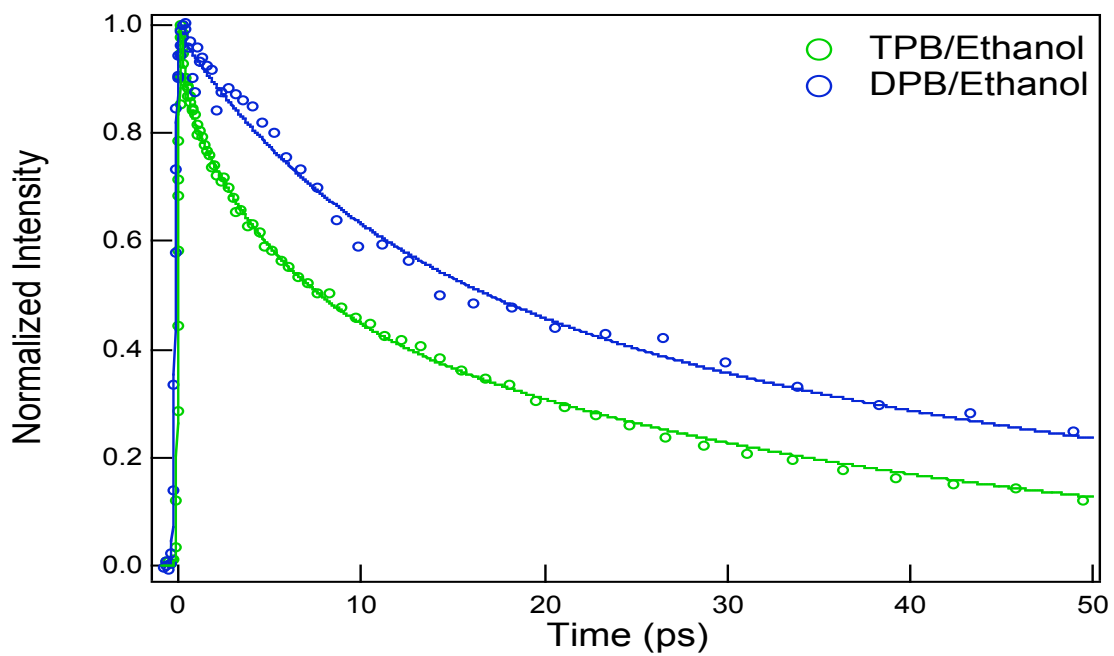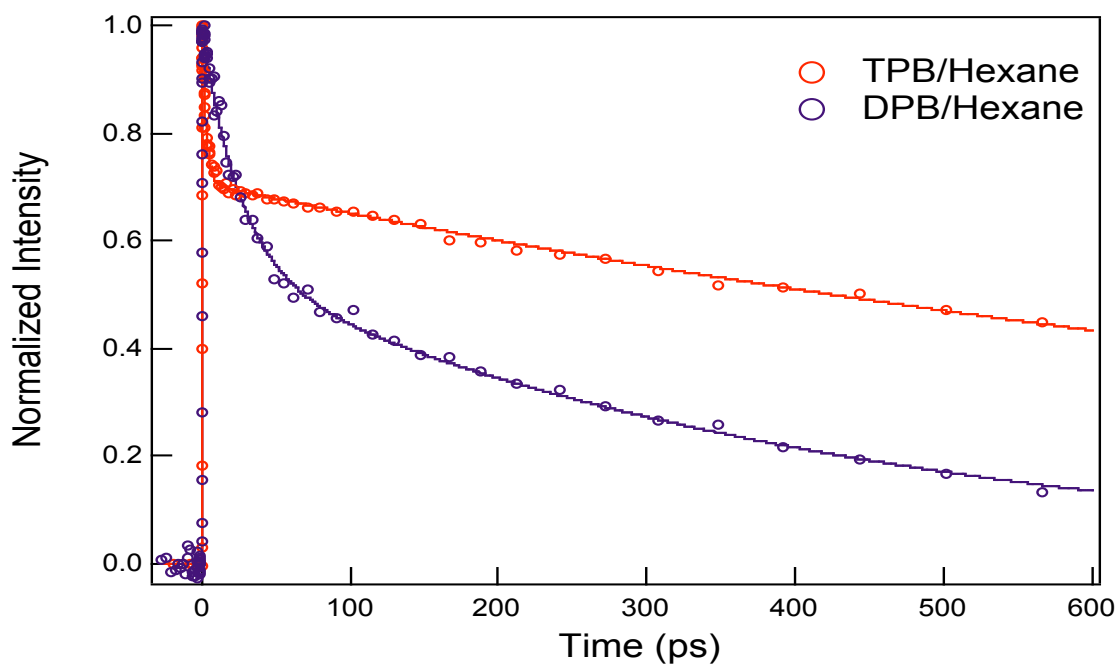
Figure 3.8. Transient absorption lifetime decays of TPB and DPB in hexane. The pump wavelengths used were 385 nm and 350 nm, respectively, with probe wavelengths of 650 nm and 630 nm, respectively. The solid lines are the best fit lines to the decays. Both decays were fit to double-exponential decays.

Molecule		τ_1 (ps)	τ_2 (ps)	τ_3 (ps)
TPB (385 nm)	Methanol	0.10 ± 0.02	1.3 ± 0.2	12 ± 1
	Ethanol	0.21 ± 0.03	4.6 ± 0.3	34 ± 1
	Hexanol	0.25 ± 0.05	13.3 ± 0.6	226 ± 4
	Decanol	1.8 ± 0.2	32 ± 2	596 ± 8
TPB (295 nm)	Methanol	0.5 ± 0.1	5 ± 1	17 ± 2
	Ethanol	0.4 ± 0.1	5 ± 1	40 ± 2
	Hexanol	0.3 ± 0.1	12 ± 2	291 ± 13
	Decanol	1.1 ± 0.1	27 ± 3	674 ± 26
DPB (350 nm)	Methanol	-	5 ± 3	25 ± 2
	Ethanol	-	9 ± 3	54 ± 13
	Hexanol	-	33 ± 7	183 ± 29
	Decanol	-	45 ± 8	325 ± 78
DPB (310 nm)	Methanol	-	3 ± 1	29 ± 5
	Hexanol	-	43 ± 8	195 ± 21

Table 3.1. Transient absorption lifetimes for TPB and DPB in alcohol solvents along with error in the fit.

Molecule		τ_1 (ps)	τ_2 (ps)	τ_3 (ps)
TPB (385 nm)	Hexane	-	2.7 ± 0.1	1189 ± 13
	Heptane	-	3.1 ± 0.1	1384 ± 21
	Octane	-	3.8 ± 0.1	1463 ± 15
	Decane	-	5.2 ± 0.2	1380 ± 20
TPB (295 nm)	Hexane	-	1.2 ± 0.1	1320 ± 30
	Heptane	-	1.3 ± 0.1	1520 ± 40
	Decane	-	1.8 ± 0.1	1740 ± 50
DPB (350 nm)	Hexane	-	25 ± 3	405 ± 42
	Octane	-	35 ± 8	550 ± 80
	Decane	-	35 ± 3	590 ± 22
DPB (310 nm)	Hexane	-	42 ± 10	434 ± 26

Table 3.2. Transient absorption lifetimes for TPB and DPB in alkane solvents along with error in the fit.

3.3 Picosecond Time-Resolved Spectroscopy

The fluorescence lifetimes for DPB in acetonitrile, ethanol, decane, decanol, hexane methanol, and octane were obtained at a pump wavelength of 290 nm and a monitor wavelength of 370 nm, which corresponds to approximately the maximum of the emission for DPB. The lifetimes of DPB in each solvent was fit to a single-exponential decay convolved with the instrument response function. Figure 3.9 shows the fluorescence decays of DPB in acetonitrile, methane, hexanol, and hexane.

The fluorescence lifetimes for TPB in hexanol, hexane, heptane, octane, and decane were obtained at a pump wavelength of 290 nm and a monitor wavelength of 430 nm, which corresponds to approximately the maximum of the emission for TPB. The fluorescence lifetimes in methanol and ethanol were too fast for the resolution of the instrument used in these experiments, and therefore, only an instrument response function was observed for these solvents. The lifetime of TPB in each solvent was fit to a single-exponential decay convolved with the instrument response function. Figure 3.10 shows the fluorescence decays of TPB in hexanol, hexane, heptane, octance, and decane.

Table 3.3 gives a comparison of the fluorescence lifetimes of DPB and TPB in the various solvents. Within a homologous solvent series, the lifetime of each molecule increases with increasing viscosity. The fluorescence lifetimes obtained for DPB and TPB correspond well with the longer lifetime component of the double-exponential and triple-exponential, transient lifetime decays, respectively.

Table 3.4 shows a comparison of the relative amplitudes of τ_2 to τ_3. At higher pump energy, it can be seen the τ_2 process becomes a larger percentage of the ratio. Table 3.5 shows a

comparison of the τ_2 and τ_3 lifetimes at each pump wavelength. It can be seen that τ_2 is shorter

at a pump wavelength of 295 nm, while τ_3 is shorter at 385 nm.
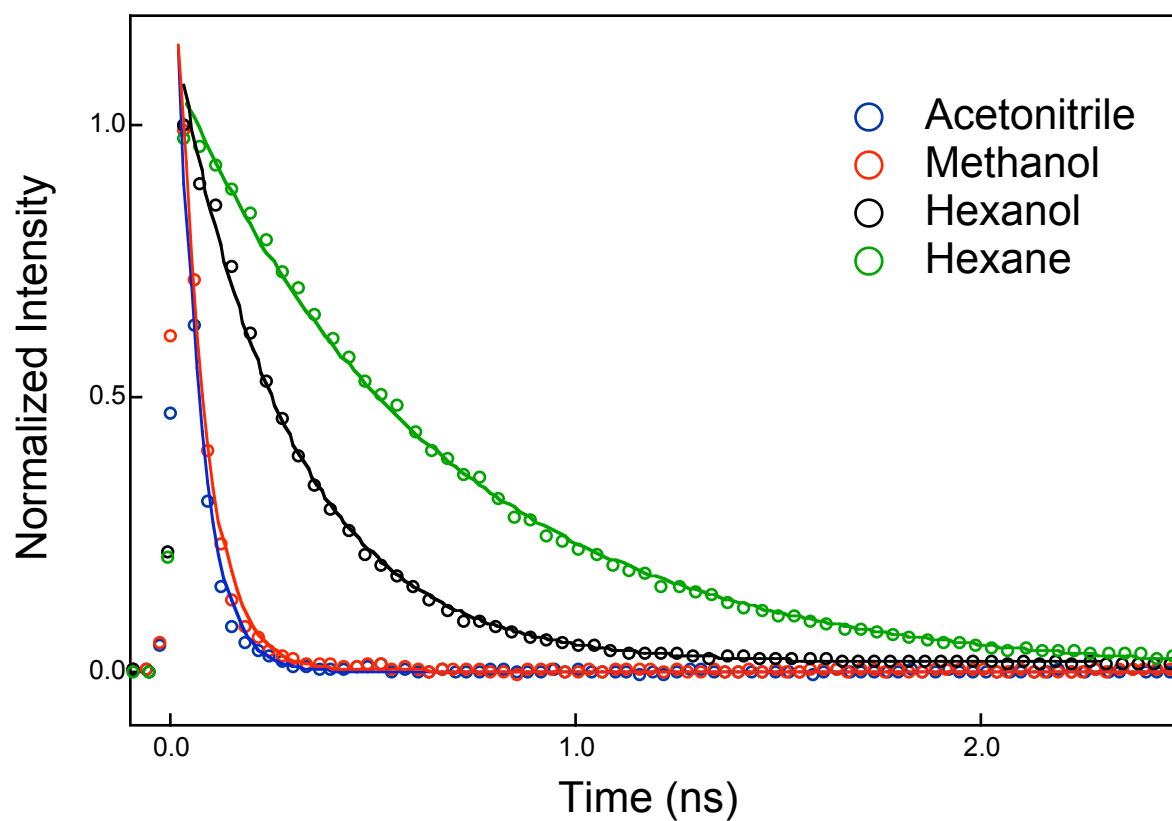
Figure 3.9. Fluorescence lifetime decays of DPB in acetonitrile, methanol, hexanol, and hexane. The pump wavelength used was 290 nm, with a monitor wavelength 370 nm. The solid lines are the best fit lines to the decays. All decays were fit to single-exponential decays.
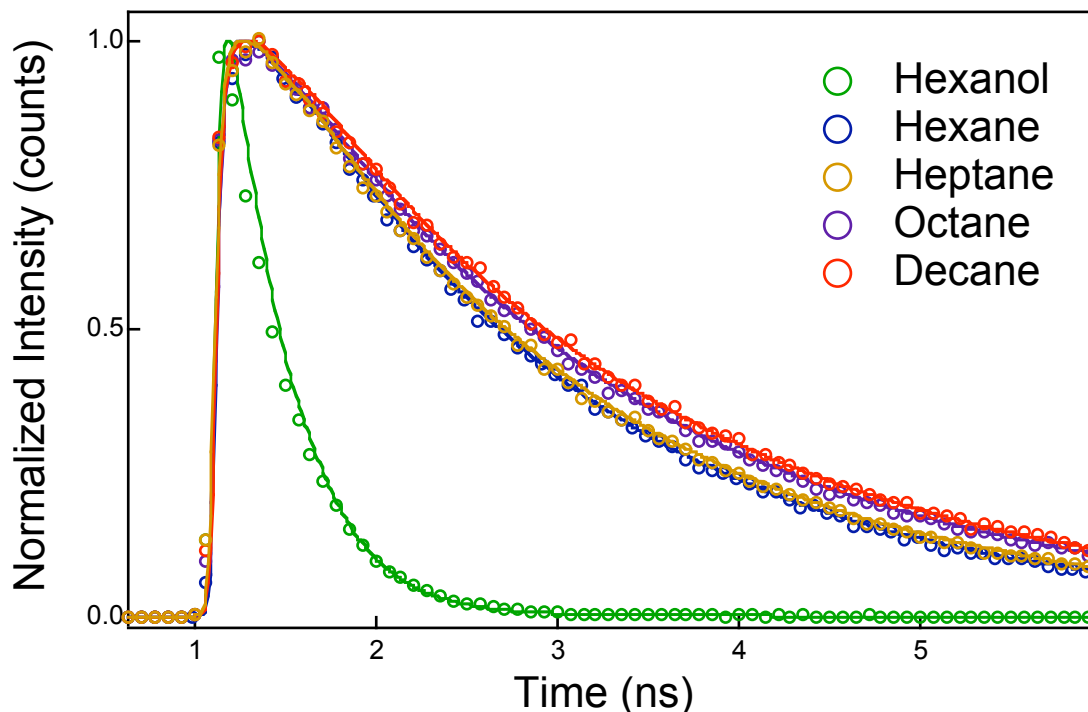
Figure 3.10. Fluorescence lifetime decays of TPB in hexanol, hexane, heptane, octane, and decane. The pump wavelength used was 290 nm, with a monitor wavelength 4300 nm. The solid lines are the best fit lines to the decays. All decays were fit to single-exponential decays.

DPB Fluorescence Lifetimes

Solvent	τ_F (ps)	Solvent	τ_F (ps)
Methanol	33 ± 1	*Hexane*	550 ± 4
Ethanol	58 ± 1	*Octane*	625 ± 2
Hexanol	223 ± 1	*Decane*	693 ± 4
Decanol	370 ± 3		

TPB Fluorescence Lifetimes

Solvent	τ_F (ps)	Solvent	τ_F (ps)
Hexanol	301 ± 1	*Hexane*	1746 ± 4
		Heptane	1812 ± 4
		Octane	2007 ± 1
		Decane	2062 ± 1

Table 3.3. Fluorescence lifetimes for TPB and DPB in alcohol and alkane solvents along with error in the fit.

	α_2/α_3	
Solvent	**385 nm**	**295 nm**
Hexane	0.47	0.97
Decane	0.46	0.75
Ethanol	0.69	0.63
Decanol	0.44	0.65

Table 3.4. Relative amplitudes of τ_2 and τ_3 for TPB in alcohol and alkane solvents.

	Lifetime			
	385 nm		**295 nm**	
Solvent	**τ_2 (ps)**	**τ_3 (ps)**	**τ_2 (ps)**	**τ_3 (ps)**
Hexane	2.7	1189	1.2	1320
Decane	5.2	1380	1.8	1740
Ethanol	4.6	34	5	40
Decanol	32	596	27	674

Table 3.4. Lifetimes of τ_2 and τ_3 for TPB in alcohol and alkane solvents.

Chapter 4

DISCUSSION

4.1 Steady-State Spectroscopy

The absorption, emission, and transient absorption of TPB are slightly red-shifted n comparison to DPB. This is a result of the two additional phenyl rings of TPB. Through these additional phenyl rings, the effective conjugation of the molecule is increased. In order to understand the reason for the red-shifted spectra, one must consider the quantum mechanical particle-in-a-box. By increasing the effective conjugation of the molecule, the electrons of TPB are given a "bigger box" in which to move about. By increasing the length of the box, the energies levels inside move lower energies. This results in spectra shifted to the red edge for the absorption, emission, and transient absorption processes.

4.2 Femtosecond and Picosecond Time-Resolved Spectroscopy

In DPB, double-exponential decay behavior was seen in the transient absorption upon excitation from both the red (350 nm) and blue (310 nm) edge of the absorption spectrum. Moller and co-workers did not previously observe this behavior. In their work, double-exponential decays were only seen upon excitation at the red edge of the spectrum. They attributed the short time component of the decay to the s-*trans* isomer and the long time component to the s-*cis* isomer[18]. The data collected for this thesis, however, do not support this view.

Only single-exponential decay behavior is observed in the fluorescence lifetime experiments for DPB. Dahl *et al.* have observed similar lifetimes for DPB in hexane. They attribute this lifetime to the ^1A_g state of DPB[19]. The long time components of the collected

transient absorption lifetimes correspond to the fluorescence lifetime experiments. For this reason, we propose these two time components arise from the same state. However, we believe this state is different than the one observed from the short time components of the double-exponential decays.

We propose the short time components arise from the 1^1B_u state. This state is known to have two competing decay pathways making it short lived. The first pathway is that of radiative decay. This pathway occurs through the symmetry-allowed transition from the excited state back to the ground state. This transition is observed as fluorescence. The non-radiative decay pathway is through isomerization from the excited state[15]. We propose the long time components of the transient absorption and fluorescence decays arise from the 2^1A_g state. This state lacks a photoisomerization pathway and transition from this state back to the ground state is symmetry forbidden, making this a longer-lived state.

The first two excited states of TPB are of B and A character. Because these states are similar in electronic properties to those of the B_u and A_g states, comparisons to the excited state dynamics of DPB can be used in order to understand the excited state dynamics of TPB.

The transient absorption lifetime decays reveal TPB exhibits excited state dynamics that are highly environment dependent. In the alkane solvent series, only double-exponential decay behavior can be seen in TPB at excitation from both the red (385 nm) and blue (295 nm) edge of the absorption spectrum. However, in the alcohol solvent series, triple-exponential decay behavior reveals an instrument limited, ultra-fast time component present in the excited state dynamics of TPB.

We attribute this ultra-fast time component (τ_1) to a longitudinal relaxation of the solvent. Upon excitation to the excited state, the nuclear geometry of TPB is not changed, according to

the Born-Oppenheimer approximation. However, the electron cloud redistributes in TPB, which forces the solvent to adjust. This time component is only seen in the alcohol series as a result of a defined solvent network of hydrogen bonds not present in the alkanes.

The second (τ_2) and third (τ_3) time components in the transient absorption decays of TPB are very similar to those observed for DPB. This suggests these processes may arise from electronic states that are similar in character to those in DPB. The τ_3 components of the transient absorption lifetimes of TPB correspond to the fluorescence lifetime experiments. For these reasons, we attribute these time components, τ_2 and τ_3, to the lifetime of the B and A symmetry states of TPB, respectively. τ_3 is longer lived due its symmetry forbidden transition back to the molecule's ground state.

The trends observed in the relative amplitudes of τ_2 and τ_3 offer insight to the movement of the excited state population. From the collected data, we can see that the τ_2 process becomes increasingly more important at pump wavelengths of higher energy. Our previous assignment has labeled this process the lifetime of the B state. This transition is much faster in TPB than in DPB and shows a clear dependence on solvent viscosity. For these reasons, we attribute this time component to a volume-conserving isomerization process. We believe the amplitude data suggests there is an energy barrier for this process that the excited state population cannot easily surmount at lower pump energies. Only when the molecule is excited to higher excited state vibrational levels can a large amount of the population access this decay pathway. At lower pump energies, the dominant pathway appears to be through internal conversion to the A state, followed by a symmetry-forbidden fluorescence transition back to the ground state. We believe this process too shows an energy barrier, due to the lifetime dependence on solvent viscosity. These processes are shown graphically in Figures 4. 1 and 4.2.
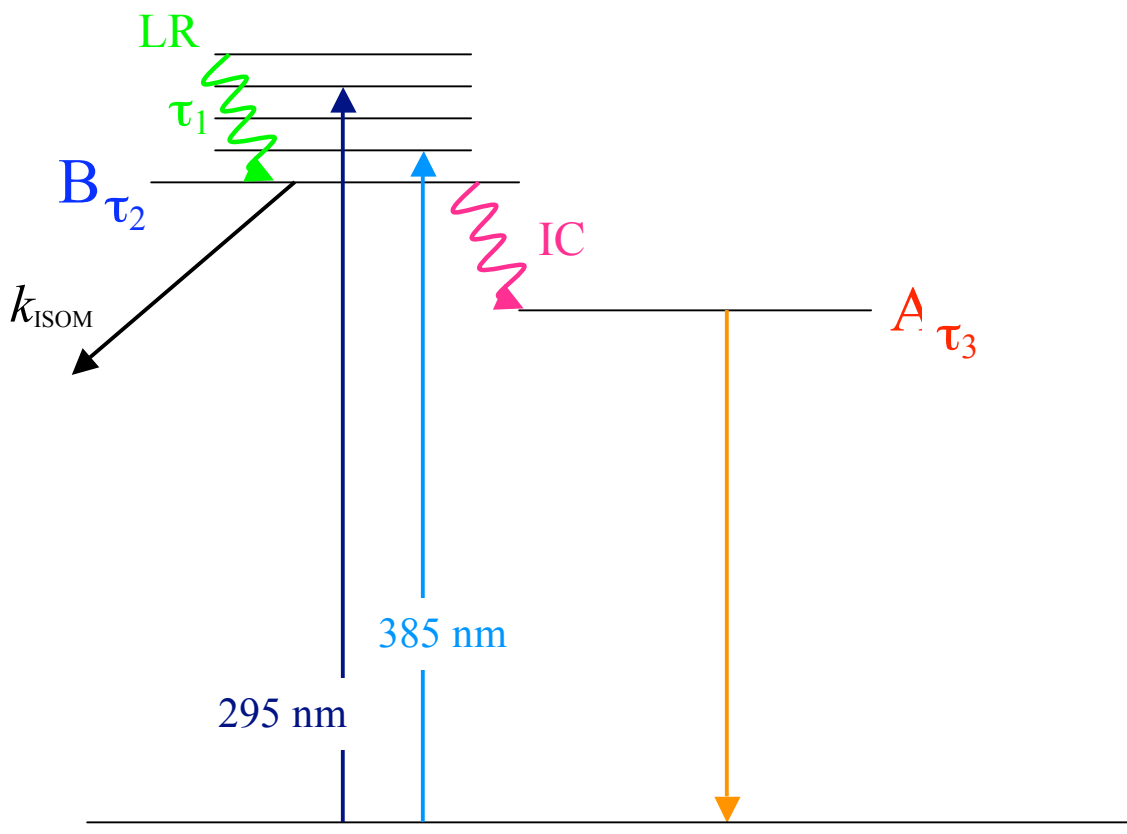
Figure 4.1. Illustration of the competing decay mechanisms for TPB. τ_1 is attributed to a longitudinal relaxation of the solvent. τ_2 is attributed to the lifetime of the B state. τ_3 is attributed to the lifetime of the A state.
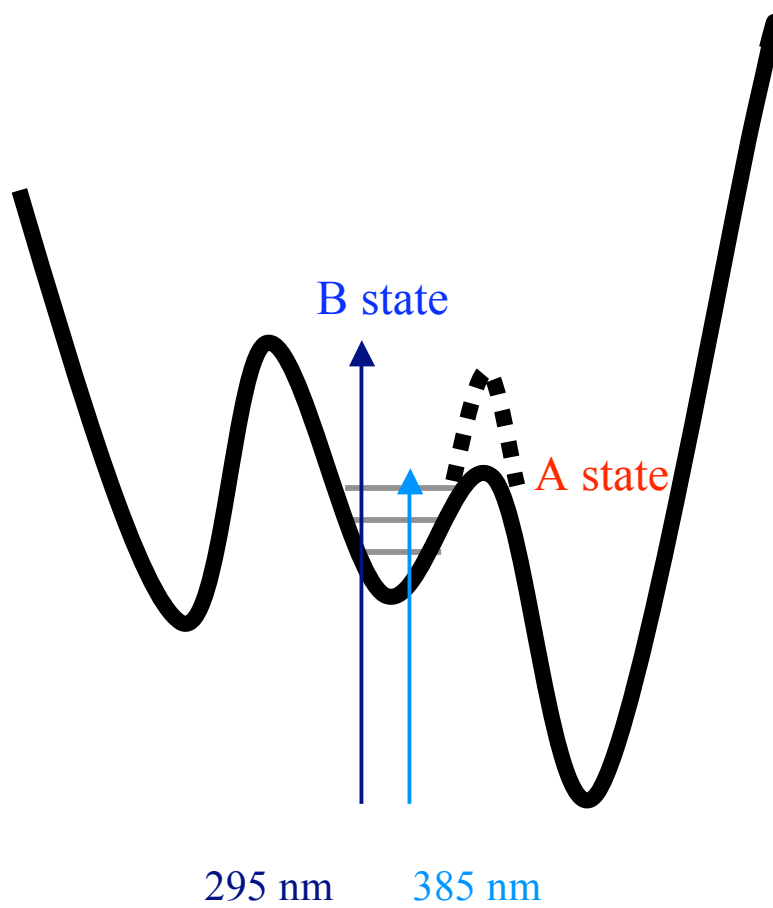
Figure 4.2. Illustration of the competing decay mechanisms for TPB considering relative amplitude data.

Chapter 5

CONCLUSIONS

Double-exponential decay behavior was observed in the transient absorption lifetimes for DPB. Fluorescence lifetime experiments revealed single-exponential decay behavior. From these results, the short time component of the transient absorption lifetime was attributed to the B_u state, while the long time component was attributed to the A_g state. Triple-exponential decay behavior was observed in the transient absorption lifetime for TPB, resulting in the first observation of the femtosecond and picosecond time components of this molecule's excited state dynamics. The shortest time component was attributed to a longitudinal relaxation of the solvent. The second time component was attributed to the lifetime of the B state, which we attribute to a volume-conserving isomerization process. The longest time component was attributed to the lifetime of the A state, which we attribute to fluorescence. The relative amplitudes of the time constants show the isomerization process from the B state becomes increasingly important at higher pump energies, suggesting an energy barrier not surmountable at lower pump energies.

Chapter 6

FUTURE WORK

The work done for this thesis provides a strong foundation for future work on the excited state dynamics of TPB. The relative amplitude of the time components of the transient absorption lifetimes should be analyzed to understand the trends of the population in each state. Decay data at more pump and probe wavelengths would offer a comprehensive view of the excited state dynamics. Fluorescence up-conversion experiments should also be preformed in order to observe and measure the ultra-fast emitting state(s) of TPB. Lastly, substituted-TPB studies would allow for identification of the photoisomerization products, thereby aiding in the assignment of a volume-conserving isomerization mechanism experienced by TPB.

References List

1. MIT Open Courseware: Biology 7.342. http://ocw.mit.edu (accessed April 22, 2009).

2. Schoenlein, R. W.; Peteanu, L. A.; Mathies, R. A.; Shank, C. V. *Science* **1991,** *254*, 412.

3. Yan, M.; Manor, D.; Weng, G.; Chao, H.; Rothberg, L.; Jedju, T. M.; Alfano, R. R.; Callender, R. H. *Proc. Natl. Acad. Sci. USA* **1991**, *88*, 9809.

4. Logunov, S. L.; Song, L; El-Sayed, M. A. Excited-State Dynamics of a Protonated Retinal Schiff Base in Solution. 100 ed.; 1996; pp 18586.

5. Warshel, A. *Nature* **1976**, *260*, 679.

6. Liu, R. S. H.; Asto, A. E. *Proc. Natl. Acad. Sci. USA* **1985**, *82*, 259.

7. Saltiel, J.; Krishna, T. S. R.; Clark, R. J. *J. Phys. Chem. A* **2006**, *110*, 1694.

8. Liu, R. S. H.; Hammond, G. S. *PNAS* **2000**, *97*, 11153.

9. Liu, R. S. H.; Hammond, G. S. *Chem. Eur. J.* **2001**, *7*, 4537.

10. Shepanski, J. F.; Keelan, B. W.; Zewail, A. H. *Chem. Phys. Lett.* **1983**, *103*, 9.

11. Velsko, S. P.; Fleming, G. R. *J. Chem. Phys.* **1982**, *76*, 3553.

12. Morris, D. L.; Gustafson, T. L. *J. Phys. Chem.* **1994**, *98*, 6725.

13. Morris, D. L.; Gustafson, T. L. *App. Phys. B* **1994**, *98*, 6725.

14. Dinur, U.; Hemley, R. J.; Karplus, M. *J. Phys. Chem.* **1983**, *87*, 924.

15. Dickson, N. M. MS Thesis, The Ohio State University, 2008.

16. El-Bayoumi, M. A.; Halim, F. M. A. *J. Chem. Phys.* **1968**, *48*, 2536.

17. Rucker, R. L.; Schwartz, B. J.; El-Bayoumi, M. A.; Harris, C. B. *Chem. Phys. Lett.* **1995**, *235*, 471.

18. Moller, S.; Yee, W. A.; GOldbeck, R. A.; Wallace-Willams, S. E.; Lewis, J. W.; Kliger, D. S. *Chem. Phys. Lett.* **1995**, *243*, 579.

19. Dahl, K.; Biswas, R.; Maroncelli, M. *J. Phys. Chem. B* **2003**, *107*, 7838.